DINAME 2017 - Proceedings of the XVII International Symposium on Dynamic Problems of Mechanics
A. T. Fleury, D. A. Rade, P. R. G. Kurka (Editors), ABCM, São Sebastião, SP, Brazil, March 5-10, 2017

Active control on drilling systems to reduce stick-slip

Guilherme R. de Paula[1], **Hans I Weber**[1]

[1] PUC-Rio, Rua Marquês de S. Vicente, 225, Rio de Janeiro-RJ, Brazil, guirsp@gmail.com, hans@puc-rio.br

Abstract: Systems actuated trough a flexible shaft poses a big challenge to control strategies as the actuator is not connected directly to the end effector, causing propagation effects as well as an energy accumulation and dissipation in the shaft. This paper focus the study in one of the most investigated application of this type, the top driven drilling system used in the oil and gas industry. Usually, the drilling system is composed by a top drive linked to the drill bit trough hundreds or even thousands of meters of steel pipes. All kind of vibrations will be found: longitudinal deformations will be associated to the bit bouncing, flexional with rubbing, and torsional with stick-slip effects. A better understanding is only possible when each of these situations is carefully investigated.This paper focuses on the torsional deformation of the highly flexible string and presents two different models for the the drill string, the first is the most common single spring single damper model. The second one is a 20 DOF Lumped parameters that has the advantage of being able to consider the mass of the drill string and propagation of torsional waves on the shaft. The investigation includes the development of a test rig adequate for torsional vibrations under damping that may induce stick-slip in the system.

Keywords: stick-slip, torsional vibrations, friction, control, drilling.

INTRODUCTION

Top driven drilling used in the oil and gas industry is one of the most investigated application of systems driven by a highly flexible shaft. These systems pose a big challenge to control strategies, as the actuator is not linked directly to the end effector, causing propagation effects as well as an energy accumulation and dissipation in the shaft. These drilling systems are composed by a top drive linked to the drill bit trough hundreds of meters of steel pipes. Drilling is one of the most expensive parts of oil prospecting and involves many risks of accidents, even though the methods in use are still very much based on trial and error experiences. Linear control theories for example, PID have little success on real drilling applications because there are lots of uncertainties present, friction with the well, friction between rock and bit, etc. This paper will present a numerical and experimental study of a few control techniques that aim to maintain a constant speed on the bit of a simple model of an oil drilling rig. A 3m long test bench Fig.1 composed by a DC motor, an elongated quite flexible shaft and a driven inertia that simulates the bit of a drilling structure, was constructed to test in the lab the controller in the presence of uncertainties and sensor noises.

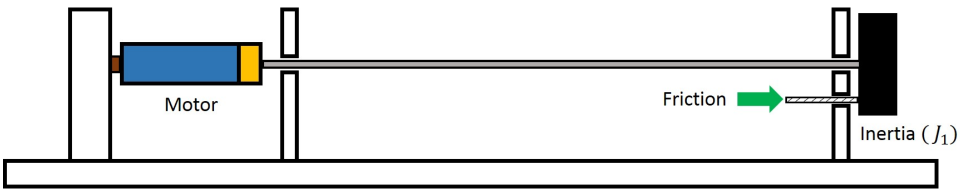

Figure 1: Test bench

The system was initially modeled as a 2 DOF torsional spring with the electrical and mechanical parts of the DC motor. This simplistic model has been proved adequate to model the test bench used, and simple enough to be applied to model reference type controllers without compromising computational effort. Another model with 20 DOF discretization of the flexible shaft was tested in order to obtain a more complete but more complex model of the system. The contact between bit and rock is modeled as sum of a Coulomb static friction coefficient, a dynamic coefficient and a viscous friction, dependent of the angular speed.

NUMERICAL MODEL

The problem of modelling the torsional dynamics of a flexible shaft can be approached in different ways. From that, only two different models were studied on this paper, one with concentrated parameters, a 2 DOF torsional mass-spring system considering only the mechanical part of the top drive motor. This model can provide fast simulations with a good description of the problem, it is also used as the reference model for Model Reference Adaptive Controllers i.e. MRAC without compromising computational effort (Hovakimyan and Cao, 2010). The model was written in the state-space form with the A matrix and the state vector x described in Eq.(1).

$$A = \begin{bmatrix} \frac{-b_1}{J_1} & \frac{K}{J_1} & 0 \\ -1 & 0 & 1 \\ 0 & \frac{-K}{J_m} & \frac{-b_m}{J_m} \end{bmatrix} \quad B = \begin{bmatrix} \frac{-Tr}{J_1} \\ 0 \\ \frac{T_m}{J_m} \end{bmatrix} \quad x = \begin{bmatrix} \dot{\theta}_1 \\ \theta_m - \theta_1 \\ \dot{\theta}_m \end{bmatrix} \tag{1}$$

where b_1 and J_1 are the bearing friction on the inertia J_1, and the inertia value. K, is the drill string torsional constant, T_m and T_r are the torque on the motor and the reaction torque, b_m is the bearing viscous friction on the motor, and J_m is the motor inertia . $\dot{\theta}_m$ is the angular speed of the motor and $\dot{\theta}_1$ is the angular speed of J_1.

The second model is a 20 DOF Lumped parameters flexible shaft Fig. 2, that was used to obtain a more complete and therefore more complex model of the system. This model also uses a complete DC motor model with electrical and mechanical parts (Svejda, 2009).

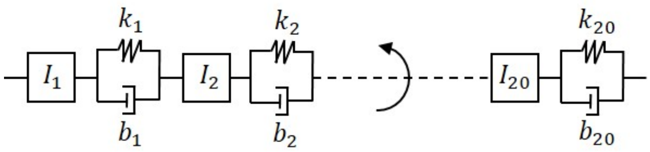

Figure 2: Lumped parameters flexible shaft

The DC motor is modeled by the equations of the mechanical Eq.(2) and electrical parts Eq.(3) as well as the torque constant k_t that is the relation between t_m and i. All the parameters used for the motor were the ones obtained by (Andrade 2013).

$$J_m \frac{d^2\theta}{dt^2} = T_m - b_m \frac{d\theta}{dt} \tag{2}$$

$$L\frac{di}{dt} = -Ri + V - e \tag{3}$$

In the lumped parameters model, each element or DOF is an ellemetary inertia-damper-spring system modeled as:

$$I\frac{d^2\theta}{dt^2} = -k\theta - b\frac{d\theta}{dt} \tag{4}$$

Writing the differential equations in Eq. (4) for each sub system and assembling them in a matrix form it becomes:

$$\bar{M}\ddot{\theta} + \bar{B}\dot{\theta} + \bar{K}\theta = \bar{\tau} \tag{5}$$

where $\bar{\theta}$ is the state vector representing the angular displacements of the lumped masses, $\bar{\tau}$ is the external torques vector,, the mass matrix ($\bar{M}$), the damping matrix ($\bar{B}$), and the spring matrix ($\bar{K}$) are:

$$\bar{M} = \begin{bmatrix} J_1 & & & & \\ & J_2 & & & \\ & & \ddots & & \\ & & & J_{19} & \\ & & & & J_m \end{bmatrix} \bar{B} = \begin{bmatrix} b_1 & -b_1 & & & \\ -b_1 & (b_1+b_2) & -b_2 & & \\ & -b_2 & \ddots & & \\ & & & (b_{18}-b_m) & -b_m \\ & & & -b_m & b_m \end{bmatrix} \tag{6}$$

$$\bar{K} = \begin{bmatrix} k_1 & -k_1 & & & \\ -k_1 & (k_1+k_2) & -k_2 & & \\ & -k_2 & \ddots & & \\ & & & (k_{18}-k_{19}) & -k_{19} \\ & & & -k_{19} & k_{19} \end{bmatrix} \tag{7}$$

This way, the mechanical lumped parameters of the drill string can be written substituting Eq. (6) and Eq. (7) in Eq. (5). The model parameters were obtained experimentally, Tab. 1 shows the numerical values.

Table 1: Model parameters used on simulations

Properties	Value	Unit
String length (L)	1.7	m
String diameter (mm)	3	mm
Total inertia of J_1	0.01555819	kgm^2
String stiffness (K)	0.2548	Nm/rad
Moment of inertia of motor (J_m)	0.37×10^{-3}	kgm^2
Armature inductance (L_{DC})	1.10×10^{-3}	H
Armature resistance (R_{DC})	0.33	Ω
Torque constant (K_t)	0.12	Nm/A
Speed constant (K_e)	6.02×10^{-2}	$V/(rad/s)$

Torque on bit formulation

The contact between bit and rock is modeled, according to (Armstrong and De Wit, 1995) and (Perneder et al., 2012) by the sum of a Coulomb static friction coefficient, a dynamic coefficient and a viscous friction, dependent of the angular speed. This contact appears on the model in the inertia J_1.

$$T_r = (T_C + (T_{brk} - T_C) \cdot exp(-c_v|\omega|))sign(\omega) + f\omega \tag{8}$$

where: T_r is the friction torque, T_C is the Coulomb friction torque, T_{brk} is the static friction torque, c_v is the dynamic friction coefficients, ω is the angular speed, and f is the viscous friction coefficient.

Wave propagation equation

The wave propagation equations as described in (Rossing and Fletcher, 2013), can be written for an uni-dimensional drill string of total length L_s by the equation Eq. (9)

$$\frac{\partial^2\theta(l,t)}{\partial t^2} = v_{tw}^2 \frac{\partial^2\theta(x,l)}{\partial x^2} \tag{9}$$

where l is the distance from the motor, θ is the angular displacement, and v_{tw} is the speed of the traveling wave. The boundary conditions for the junction with the top drive and for the junction with the BHA (J_1), are derived from the angular momentum and include the motor and friction on bit characteristics. As the friction characteristic is strongly nonlinear, an analytic solution for this continuous model is not possible (Kreuzer and Steidl, 2012).

SIMULATION ANALYSIS

Simulations described in this work were performed in Matlab/Simulink environment. As the 20 DOF lumped masses model is more complete and in this paper model reference controllers will not be addressed, this 20 DOF model will be the base for all the simulations described. A step of angular velocity at $t = 0$ is applied on the top drive motor. Is possible to observe the torque and the angular speed of J_1 for the model with Fig. 4, and without Fig. 3 the dry friction Eq.(8) applied in J_1.

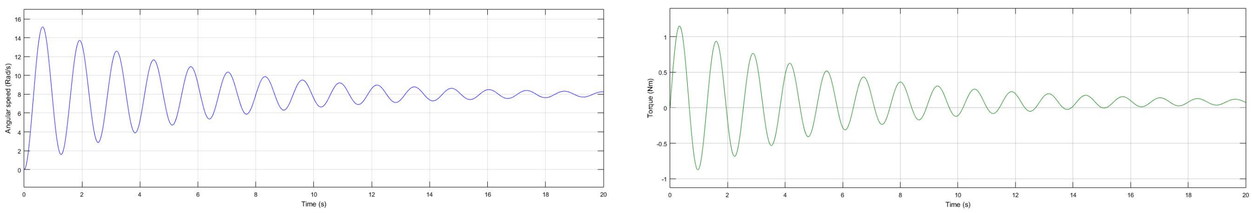

(a) Angular speed without dry friction

(b) Torque without dry friction

Figure 3: Simulation of the system without dry friction, Angular speed (a) and Torque applied by motor (b)

It is possible to see that the stick-slip appears due to the dry friction introduction on J_1 and, as expected, with the increase on the friction, the necessary torque on the top drive motor increases substantially to maintain the same angular speed.

After observing that the model can describe effectively the effects of the stick-slip a PID controller was designed and tuned using MATLAB PID Tunner app applied on a linearized plant, with the fine tuning done by hand observing the results achieved. Simulations were performed to analyse the results of the implementation of a simple linear control on a model that is highly non linear due to the dry friction applied. The proposed mathematical methods to obtain the optimum PID gains are suited for a linear plant witch is not the case. Figure 5 shows the block representation of the control, being the observed state the angular speed in J_1 and the controlled parameter the top drive angular speed ($\dot{\theta}_m$).

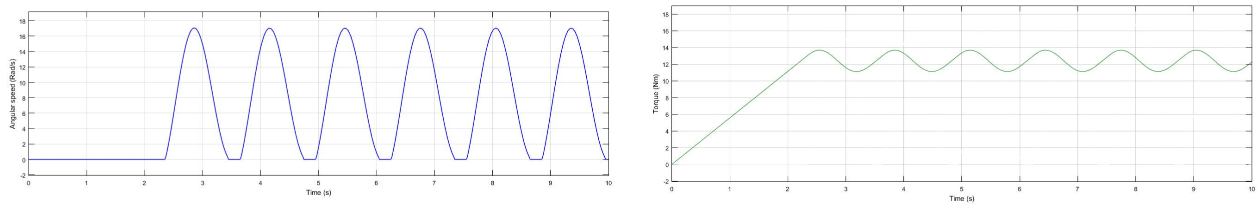

(a) Angular speed with dry friction

(b) Torque with dry friction

Figure 4: Simulation of the system with dry friction, Angular speed (a) and Torque applied by motor (b)

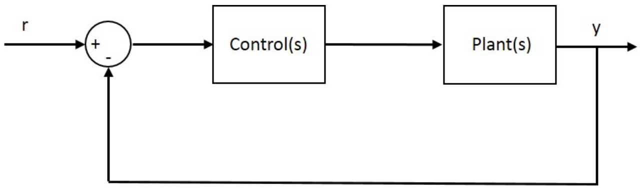

Figure 5: PID control structure

The results of this controller are shown in Fig. 6 for the plant without dry friction and in Fig. 6 for the plant with dry friction, showing the torque and the angular speed at J_1. The approach of using a linearized plant to tune a PID controller and then apply this gains on the non linear plant showed good results for the given conditions of this simulation.

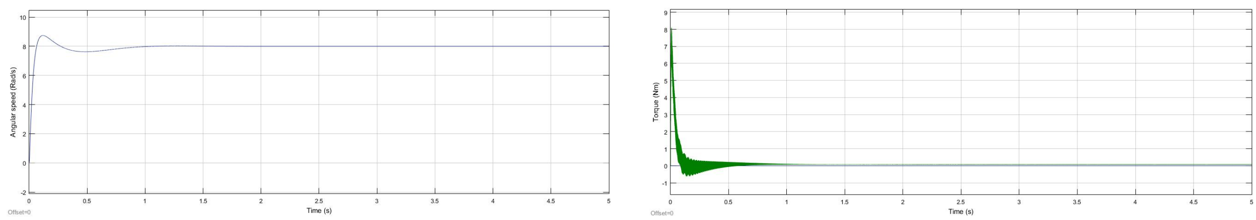

(a) Angular speed without dry friction

(b) Torque without dry friction

Figure 6: Simulation of the PID system without dry friction, Angular speed (a) and Torque applied by motor (b)

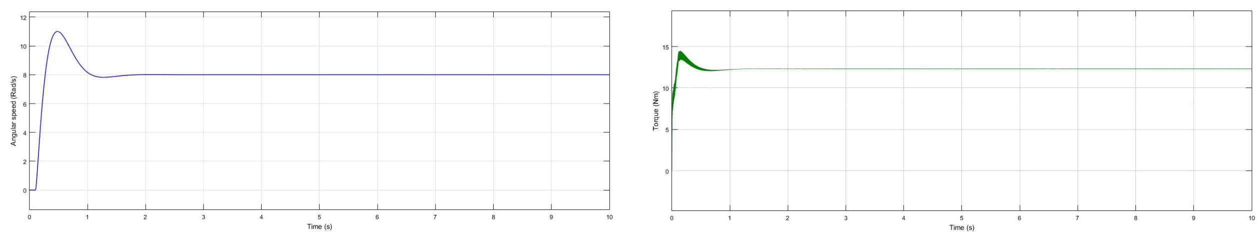

(a) Angular speed with dry friction

(b) Torque with dry friction

Figure 7: Simulation of the PID system with dry friction, Angular speed (a) and Torque applied by motor (b)

Phase signal influence on the controlability

By analyzing the structure of the friction law Eq.(8) it came the idea that by adding a torque source to J_1 (a kind of downhole motor), it could be possible to modify the stick slip phenomenon. Using this supposition it was started an analysis to verify if it is possible to mitigate the stick slip by controlling the torque on J_1. The model was then modified to add a secondary, much smaller DC motor, modeled as well by Eq. (2) and Eq. (3). Figure 8 shows a schematic of this setup.

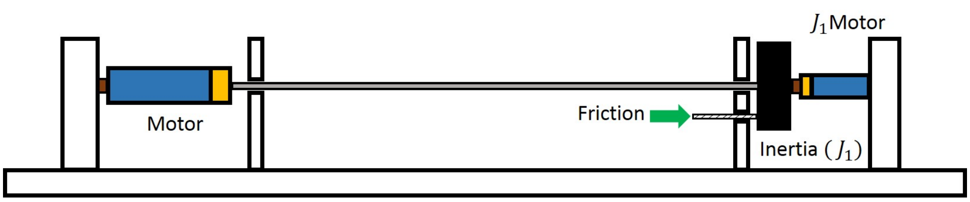

Figure 8: Test bench with DC motor on J_1

A recent study from (Shor et al., 2015), showed that the propagation effects on torsional vibrations are important for the implementation of torsional vibrations mitigation techniques, which led to suppose on a first moment that the phase of the proposed control for an imposed torque on J_1 should be important for the results. Therefore, it was simulated the lumped masses system described in section ”Numerical model”. The simulations started at $t = 0s$ with angular displacement and speed of the drill string being zero. In $t = 0$ the Top drive motor is started at 2 rad/s, at around 9s the energy accumulated on the drill string is enough to overcome the static friction force and the stick slip phenomenon begins. In $t = 15s$ a second DC motor attached to J_1 is energized applying a torque of aprox. $-0.29Nm$ to J_1. Results are shown in Fig. 9.

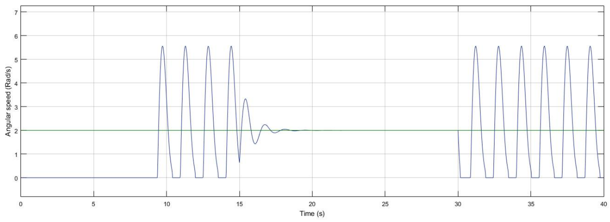

(a) Angular speed on top drive (green) and J_1(blue)

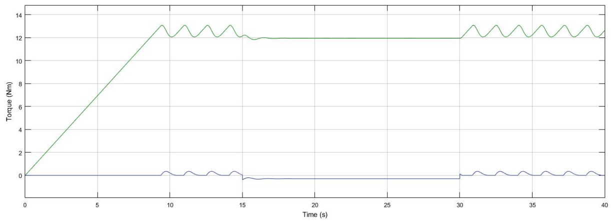

(b) Torque on top drive (green) and J_1(blue)

Figure 9: Angular speed and torque results with added torque in J_1 from 15s to 30s

As described by (Shor et al., 2015), the delay effects from the propagation of torsional vibrations along the drill string must be considered for the control structure of the problem. To prove that the developed mathematical model is capable of representing these effects, the system described in Fig. 9, was also simulated for a torque on J_1 being applied from $t = 14s$ to $t = 30s$.

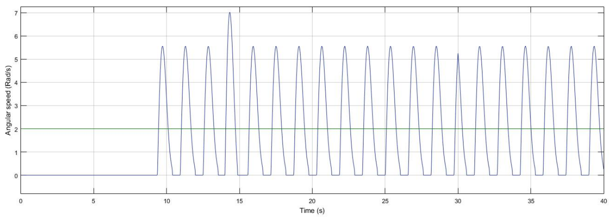

(a) Angular speed on top drive (green) and J_1(blue)

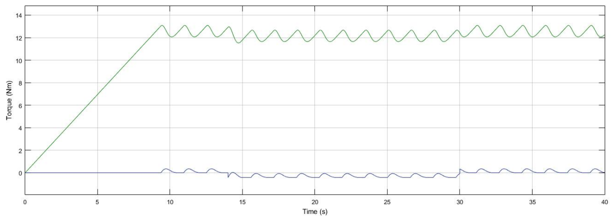

(b) Torque on top drive (green) and J_1(blue)

Figure 10: Angular speed and torque results with added torque in J_1 from 14s to 30s

Results in Fig. 10 show that if the torque on J_1 is applied in a wrong moment it will have no effect on the stick-slip, only adding a small disturbance on the angular speed when it is applied.

EXPERIMENTAL TESTS

In order to perform the experimental tests, a test bench was made Fig. 11. This apparatus is proposed to study only the rotational and torsional dynamics of the system, for that reason the motor and the inertia are mounted on bearings so that the setup can be used in an horizontal position, making it easy to operate. The drill string is 2.4m long and is made of a 3mm diameter steel rod. The DC motor is mounted on two ball bearings, so the torque applied by the motor is obtained through a force measured by a load cell positioned at a known distance from the motor. This force, the normal force of the brake on the inertia, and the rotational speed of the motor and of the inertia, are measured and these data are acquired by a National Instruments cDAQ system.

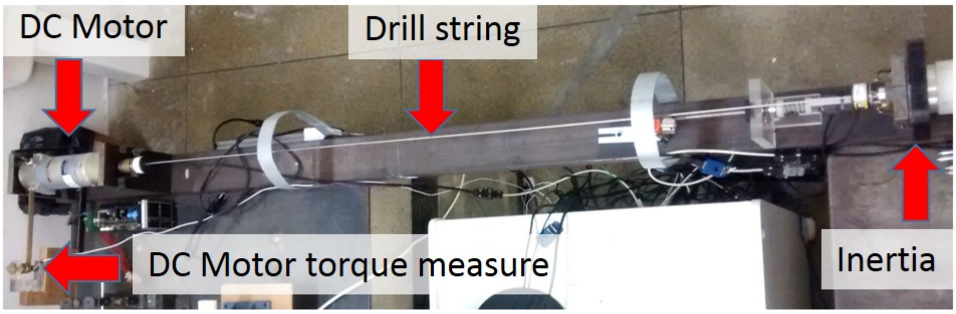

Figure 11: Experimental setup

Figure 12 shows the results obtained with the apparatus shown in Fig. 11. In blue, on the left axis is the angular speed in RPM of J_1, in orange on the right axis is the amplitude of the torque in Nm applied by the DC motor attached to

J_1. Results shown are very similar to the ones obtained with the numerical model Fig. 9. The torsional vibration on the experimental test rig is not completely eliminated due to noise on the sensors and to non-modeled imperfections of the apparatus. But this approach shows that it can eliminate the stick-slip during the period the DC motor is being used.

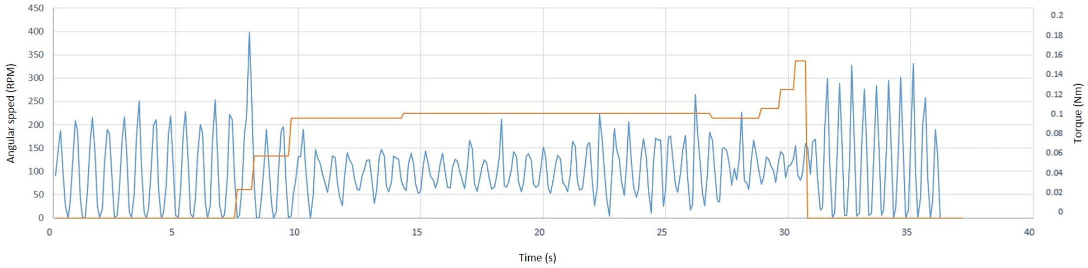

Figure 12: Experimental results for torque applied on J_1 in green and speed at J_1 in orange

Influence of top drive speed on stick-slip

The influence of the top drive speed on the behaviour of the stick-slip was analysed experimentally applying increasing steps to the top drive up to a maximum of 60 RPM and back to 0 RPM at the end. Figure 13 shows the results for experimental tests where the angular speed of J_1 is drawn in blue, the set point speed of the top drive in red and the measured speed of the top drive in orange. In this case there is no active control acting on the system, and the friction normal force is maintained constant during all the tests. It is possible to observe that the maximum speed of the bit (J_1) is constant up to 100s, i.e. varying the speed of the top drive from 20 RPM um to 40 RPM, although the behaviour of the stick slip varies, the maximum speed on the bit is very similar. On the other hand, by increasing the top drive speed from 40 to 45 RPM the maximum speed on the bit almost doubles, going from around 70 to 120 RPM. Observing the transition in 155s from 55 RPM to 60 RPM, an interesting phenomenon happens, the stick slip disappears and the amplitude of the torsional vibrations reduces.

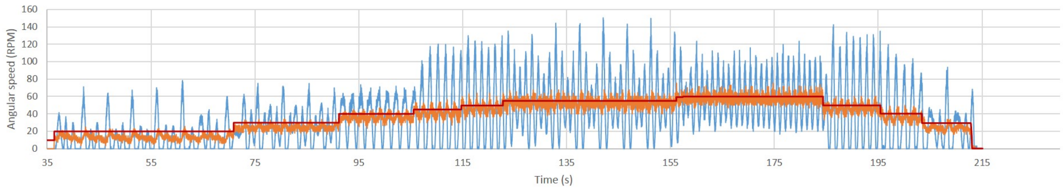

Figure 13: Influence of top drive speed on stick-slip

Experimental analysis of torsional waves propagation on the drill string

(Kreuzer and Steidl, 2012) analyses the mathematical approach of torsional wave propagation on the drill string for a full scale drill string. In the article it is stated that the travelling speed of torsional waves on the full scale drill string is $3.184(m/s)$. To measure the speed of propagation at the reduced scale setup the system was put on 0 RPM initial condition and by $t = 12.5s$ a step of 95 RPM is applied on the top drive. The angular speed of J_1 is measured and then the speed of wave propagation is calculated. The Δt measured is $0.065s$, that divided by the drill string length results in the speed $v_{tw} = 36.92m/s$

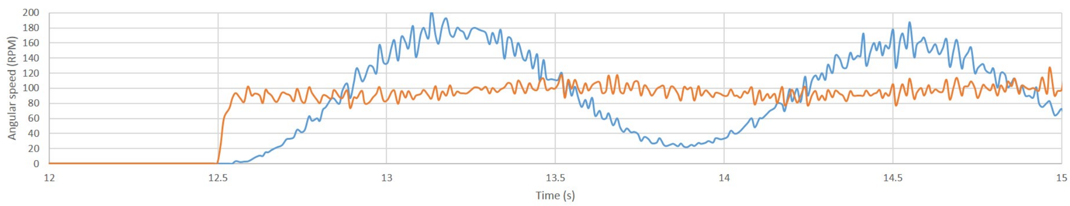

Figure 14: Step response of the system without friction on J_1

CONCLUSIONS

It was shown that it is possible to mitigate the stick-slip phenomenon by applying a small torque on the bit, orders of magnitude lower than the one applied by the main motor, i.e. top drive. Is becomes also clear that in a real system, even a reduced scale one like the apparatus presented, where the torque on bit cannot be modeled as a simple equation, the stick-slip form is highly dependent of the top drive speed, although to eliminate the stick slip by simply increasing the speed of the top drive may require a substantial increase in that speed. It was also shown that a simple PID controller tuned using a linearized plant, it turned on with the plant remaining still is able to control the stick-slip with a reasonable control effort (torque) and without increasing the angular speed. The measured traveling speed of torsional waves in the 3mm diameter steel rod used at the experimental setup, was much higher than what the literature (Rossing and Fletcher, 2013) and (Kreuzer and Steidl, 2012) registers, this can be due to the much smaller diameter than what they present in their papers, or due to the data acquisition equipment used in the tests, showing that further investigation on that mater is needed.

REFERENCES

Andrade, B., 2013, ”Numerical and experimental analysis of nonlinear torsional dynamics of a drilling system”, M.Sc. Dissertation, PUC-Rio University, Brazil.

Armstrong, B. and de Wit, C., 1995, ”Friction Modeling and Compensation”, The Control Handbook, CRC Press.

Hovakimyan, N. and Cao, C, 2010, ”L1 Adaptive Control Theory: Guaranteed Robustness with Fast Adaptation”, Series: Advances in Design and Control, Philadelphia, PA.

Kreuzer, E., Steidl, M., 2012, ”Controlling torsional vibrations of drill strings via decomposition of traveling waves”, Archive of Applied Mechanics, Volume 82, pp.515–531.

Perneder, E., Detournay, E. and Downton, G., 2012, ”Bit/rock interface laws in directional drilling”, International Journal of Rock Mechanics and Mining Sciences Trans. Commun, Volume 51, pp. 81–90.

Rossing, T. and Fletcher, N.H., 2013, ”Principles of Vibration and Sound”, 2^{nd} ed., Springer.

Svejda, M., 2009, ”Application of output tracking for DC motor with flexible shaft”, 17th International Conference on Process Control, pp.464–470.

Shor, R. J., Pehlivanturk, C., Acikmese, B., van Oort, E., 2015, ”Propagation of torsional vibrations in drillstrings: How borehole geometry affects transmission and implications on mitigation techniques”, 17th International Conference on Engineering Vibration.

RESPONSIBILITY NOTICE